Epigenome characterization at single base-pair resolution

Jorja G. Henikoff[a], Jason A. Belsky[b], Kristina Krassovsky[a,c], David M. MacAlpine[d], and Steven Henikoff[a,e]

[a]Basic Sciences Division and [e]The Howard Hughes Medical Institute, The Fred Hutchinson Cancer Research Center, Seattle, WA 98109; [b]Program in Computational Biology and Bioinformatics, Duke University, Durham, NC 27710; [c]Molecular and Cellular Biology Program, University of Washington, Seattle, WA 98195; and [d]Department of Pharmacology and Cancer Biology, Duke University Medical Center, Durham, NC 27710

Edited* by Steven E. Jacobsen, University of California, Los Angeles, CA, and approved September 30, 2011 (received for review July 6, 2011)

We have combined standard micrococcal nuclease (MNase) digestion of nuclei with a modified protocol for constructing paired-end DNA sequencing libraries to map both nucleosomes and subnucleosome-sized particles at single base-pair resolution throughout the budding yeast genome. We found that partially unwrapped nucleosomes and subnucleosome-sized particles can occupy the same position within a cell population, suggesting dynamic behavior. By varying the time of MNase digestion, we have been able to observe changes that reflect differential sensitivity of particles, including the eviction of nucleosomes. To characterize DNA-binding features of transcription factors, we plotted the length of each fragment versus its position in the genome, which defined the minimal protected region of each factor. This process led to the precise mapping of protected and exposed regions at and around binding sites, and also determination of the degree to which they are flanked by phased nucleosomes and subnucleosome-sized particles. Our protocol and mapping method provide a general strategy for epigenome characterization, including nucleosome phasing and dynamics, ATP-dependent nucleosome remodelers, and transcription factors, from a single-sequenced sample.

Saccharomyces cerevisiae | V-plot | transcription factor binding sites

Short-read deep-sequencing technologies have the potential of revolutionizing epigenomic profiling by making it possible to map DNA fragments with single base-pair resolution at reasonable cost. This ideal has been achieved for nucleosomes, which can be mapped at high resolution by treatment with micrococcal nuclease (MNase). MNase is a single strand-specific secreted glycoprotein that cleaves one strand when DNA breathes, then cleaves the other strand, resulting in a double-strand break. MNase then "nibbles" on the exposed DNA ends until it encounters an obstruction, such as a nucleosome, where the histone cores protect the DNA from further encroachment. Although MNase has long been used for studying nucleosomes (1), its mechanism of action on DNA suggests that it will stop "nibbling" at any obstruction, such as a DNA-binding protein. We had previously shown that MNase digestion of *Drosophila* nuclei followed by low-salt native chromatin extraction can be used to map both nucleosomes and paused RNA Polymerase II using paired-end sequencing (2). Similarly, Kent et al. used MNase digestion of uncrosslinked yeast nuclei to map binding sites for both nucleosomes and smaller particles identified as sequence-specific transcription factors (3). These studies showed that MNase-protected DNA fragments as small as ~50 bp could be recovered and mapped.

A limitation of using paired-end sequencing as a read-out method for MNase mapping is that standard sequencing library preparation methods are optimized for DNA fragments of a few hundred base pairs, whereas the fragments protected by DNA-binding proteins are an order-of-magnitude smaller. Here we introduce a rapid Solexa library preparation protocol that efficiently recovers particles down to ~25 bp in size but excludes primers and adapters without gel purification. We have applied this protocol to small amounts of DNA extracted from MNase-treated yeast nuclei and native chromatin, and have obtained occupancy maps that resolve nucleosomes and small subnucleosomal particles at or near single base-pair resolution. We show that dot-plots of fragment midpoint vs. length can reveal subtle chromatin features in the vicinity of transcription-factor binding sites.

Results

Modification of the Solexa Library Preparation Protocol for MNase Mapping. MNase cleaves within linker regions between nucleosomes to generate familiar ladders of mono-, di-, and oligonucleosomes (1). We and others had previously used paired-end deep sequencing to identify subnucleosomal particles (2, 3). However, the standard protocols for preparing sequencing libraries include size cutoff and clean-up steps for removing adapters and primers, which will also deplete the small DNA fragments that we were interested in profiling. Therefore, we modified the Illumina paired-end library protocol to permit efficient recovery of DNA fragments down to ~25 bp. To avoid preferential loss of small particles, improve reproducibility, and maximize yield, we eliminated all gel purification and Qiagen kit clean-up steps. Instead, we used either phenol-chloroform followed by size exclusion spin column or Ampure XP magnetic-bead clean-up steps and also minimized tube transfers. This modified protocol allowed for efficient library preparation using as little as 20 ng of starting DNA. Because the Ampure bead protocol sharply excludes DNA below 90 to 100 bp, and the Illumina paired-end adapters add a total of 66 to 67 bp to each successfully ligated fragment, a pre-PCR Ampure bead step removed unligated adapters but retained inserts above ~25 bp.

We performed MNase digestion of crude yeast nuclei for 2.5 and 20 min according to a standard protocol (4). After DNA extraction, we prepared libraries from these samples and performed paired-end sequencing for 25 cycles per end on an Illumina HiSeq 2000 Genome Analyzer, obtaining ~150 million mapped reads per sample. A histogram of mapped fragment lengths showed a narrow distribution corresponding to nucleosome-sized DNA fragments, ~165 bp for the 2.5-min digestion and ~150 bp for the 20-min digestion (Fig. 1*A*). Smaller peaks became resolved at ~90 bp and ~130 bp in the 20-min sample. In

Author contributions: J.G.H. and S.H. designed research; K.K. and S.H. performed research; J.A.B. contributed new reagents/analytic tools; J.G.H., J.A.B., D.M.M., and S.H. analyzed data; and D.M.M. and S.H. wrote the paper.

The authors declare no conflict of interest.

*This Direct Submission article had a prearranged editor.

Freely available online through the PNAS open access option.

Data deposition: The sequence reported in this paper has been deposited in the Gene Expression Omnibus (GEO) database, www.ncbi.nlm.nih.gov/geo (accession no. GSE30551).

[1]To whom correspondence should be addressed. E-mail: steveh@fhcrc.org.

This article contains supporting information online at www.pnas.org/lookup/suppl/doi:10.1073/pnas.1110731108/-/DCSupplemental.

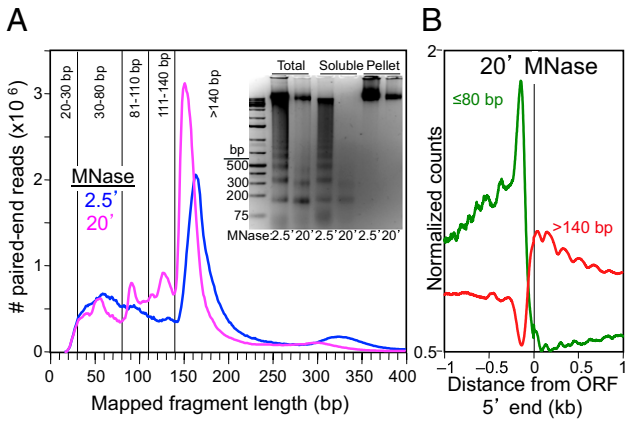

Fig. 1. Paired-end sequencing maps small MNase-protected particles. (*A*) Size distributions of mapped paired-end reads displayed as raw counts. Agarose gel analysis of MNase time-point samples (*Inset*) showing DNA from whole nuclei, soluble chromatin, and the insoluble pellet, extracted from strain Sby5146 (derived from W303: MATa leu2-3,112 his3-11:pCUP1-GFP12-LacI12:HIS3 trp1-1:256lacO:TRP1 can1-100 ade2-1 Δlys2 Δbar1 cse4ΔKan ura3-1:pCse4-3×FLAG-CSE4 + 500 bp) after MNase digestion. The band at limiting mobility is likely to be undigested genomic DNA from ∼10% of cells that retained their cell walls intact, thus preventing MNase entry. (*B*) Alignment of read data around 5′ ORF ends showing that subnucleosomal particles (≤80 bp) are enriched where nucleosomes (>140 bp) are depleted.

addition, we observed a broad distribution of mapped fragment lengths in the 30- to 80-bp range (Fig. 1*A*).

Close Packing of Distinctive Particles at Intergenic Sites. For genome-wide analysis, we divided the fragments into five size classes: <30 bp, 30 to 80 bp, 81 to 110 bp, 111 to 140 bp, and >140 bp. Within each class, we aligned the reads, and for each base-pair position we counted the number of fragments that spanned it, scaling to the total genome size such that the random expectation for each size class is 1. Strikingly, subnucleosomal particles were found to occupy nearly all intergenic regions (Fig. 2*A*). When genes were aligned at ORF boundaries we observed that subnucleosomal particles were enriched in nucleosome-depleted promoter regions (Fig. 1*B*), showing little correlation with expression level (Fig. S1) (3).

To determine whether MNase protection delimits particle boundaries, we used a low-salt (150 mM NaCl) needle-extraction procedure that thoroughly solubilizes chromatin without disrupting nucleosomes or other tightly bound particles (Fig. 1*A*, *Inset*) (5). DNA from both the soluble and the insoluble (pellet) fractions were used for paired-end sequencing. We observed nearly identical profiles for nuclear DNA, soluble chromatin, and the pellet, with all subnucleosomal features evident (especially in the pellet), where some subnucleosome-sized particles were relatively enriched (Figs. 2*B* and Fig. S2). This similarity between the total nuclear DNA, soluble chromatin, and the insoluble residue in both 2.5- and 20-min digests implies that any unoccupied DNA is rapidly digested, leaving only DNA that is tightly bound in particles.

Close examination of subnucleosome-sized particles in intergenic regions revealed evidence for multiple distinct particles occupying intergenic regions. In the representative example shown in Fig. 2*A* (*Right*), there are two well-phased nucleosomes occupying either side of an ∼200-bp intergenic region (*Bottom* tracks), and two sharply defined 20- to 30-bp particles lie inside (dotted lines). Within the 150-bp span delimited by these 20- to 30-bp peaks, a particle occupying the right half is present in both the 30- to 80-bp size class and the 81- to 110-bp size class. On the left half, a particle is present in the larger size classes, including the >140-bp class, which suggests that this is a nucleosome. To account for the presence of this putative nucleosomal DNA in size classes in which DNA from the well-phased flanking nucleosomes is absent, we propose that this nucleosome is partially unwrapped (6). Consistent with this interpretation, the

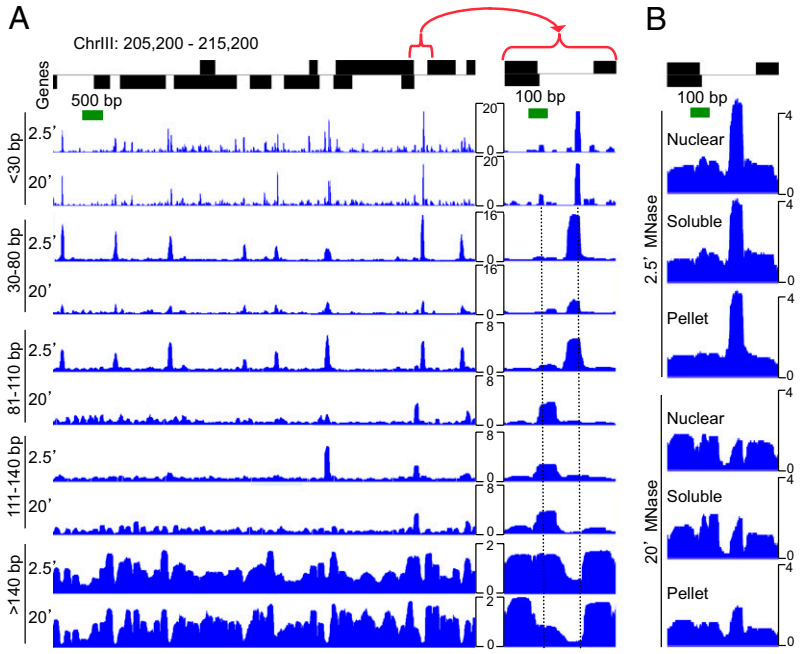

Fig. 2. MNase protection landscape for a representative region of the genome. (*A*) Mapped paired-end reads were divided into five size categories, and occupancy landscapes were obtained by counting the number of reads in a size class spanning each base pair, measured as normalized counts on the *y* axis. Differences between the 2.5- and 20-min time points are most evident for the intermediate size classes. An intergenic region is expanded on the right. ORFs on the plus (+) strand are shown above the line and on the minus (–) strand are shown below. (*B*) Nuclear, soluble, and pellet DNA samples were sequenced and profiled. Normalized counts for all size classes combined are shown for the expanded region, with the full region displayed in Fig. S2.

footprint becomes smaller with increasing digestion, as occupancy decreases in the >140-bp size class, increases slightly in the 111- to 140-bp size class and increases dramatically in the 81- to 110-bp size class. The particle of intermediate size on the right is extremely sensitive to loss during MNase digestion, as it nearly disappears from all size classes by 20-min digestion. Therefore, we see three distinct classes of particles between the two well-phased nucleosomes, ~25-bp MNase-resistant particles representing DNA-binding proteins, a partially unwrapped nucleosome, and an MNase-sensitive particle with a large footprint.

The presence of both partially unwrapped nucleosomes and nuclease-sensitive particles in the intermediate size classes might account for the conspicuous differences between the 2.5- and 20-min MNase profiles for the 81- to 110- and 111- to 140-bp size classes, but not for the others in the 10-kb representative region shown in Fig. 2*A*. To quantify this distinction, we calculated the correlations between the 2.5- and 20-min dataset occupancies over all 316,585 positions of chromosome III for the five-fragment size classes. Whereas the 2.5- and 20-min tracks were well-correlated in the 20- to 80-bp range ($r = 0.64$ for <30 bp and $r = 0.71$ for 30–80 bp) and in the >140-bp range ($r = 0.61$), correlations were very low in the 81- to 110-bp range ($r = 0.25$) and in the 111- to 140-bp range ($r = 0.15$), and similar correlations were observed for other chromosomes. We conclude that small DNA-binding proteins are well-protected from nuclease digestion, even though MNase can encroach upon particles of intermediate size and partially unwrapped nucleosomes.

Nucleosome Eviction During MNase Digestion. We suspected that many of the subnucleosomal particles that we observed were ATP-dependent nucleosome remodelers. To ascertain whether this hypothesis might be the case, we examined the Gal1-Gal10 region, where a previous study had mapped the remodel of the structure of chromatin complex (RSC) nucleosome remodeler to the Gal4 UAS (7). This study documented the presence of a single partially unwrapped nucleosome in cells grown in glucose, which we confirmed: this nucleosome is most abundant in the 111- to 140-bp size class. Furthermore, the nucleosome is especially well-positioned, in that it shows an almost perfectly square peak, in contrast to the more rounded peaks of ordinary phased nucleosomes, where intermittent unwrapping can allow encroachment by MNase (Fig. 3*A*). However, in addition, we found that its occupancy decreased drastically during MNase digestion, nearly disappearing in the 20-min sample. Remarkably, a 30- to 80-bp particle displayed the opposite behavior at the same site, showing limited MNase protection at 2.5 min, with expansion of protection as the nucleosome was evicted. This expansion is in contrast to most other examples of intergenic particles in the 30- to 80-bp fraction, where increasing digestion led to reduced protection (Fig. 2*A*), and provides evidence of occupancy of distinct particles at the same site in different individuals in the yeast cell population.

The small particle over the Gal4 UAS is likely to be the RSC, which Floer et al. have reported shows its maximal cross-linked ChIP signal for chromosome II precisely over this nucleosome in cells grown in glucose (7). The RSC is not the only subnucleosomal particle that increased in occupancy during nucleosome eviction ex vivo, and there are many similar examples that can be readily found by visually scanning profiles (Fig. S3). We infer that MNase double-strand cleavage allowed the histone core of this nucleosome to slide off the DNA, with concomitant expansion of protection by the RSC, which was initially positioned over the RSC motif identified by Floer et al. (7). This ex vivo behavior is consistent with the DNA translocase action of the RSC in evicting nucleosomes (8). Intriguingly, we also found that a minor fraction of this partially unwrapped nucleosome was insoluble after MNase treatment at both time points (Fig. 3*B*). Floer et al. had proposed that engulfment of the nucleosome by

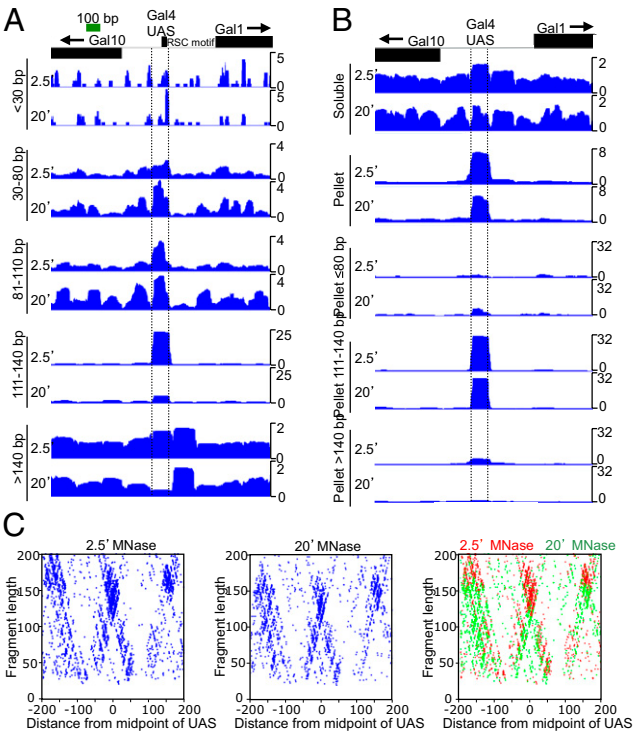

Fig. 3. MNase digestion causes nucleosome eviction and putative RSC enrichment over the Gal4 UAS ex vivo. (*A*) Subnucleosomal and nucleosomal profiles during MNase digestion of the well-studied Gal1-10 region. Note the square peak of the RSC-disrupted nucleosome most prominent in the 111- to 140-bp fraction. Both the maximum chromosome II RSC X-ChIP signal and the maximum 125-bp chromatin signal are located over the Gal4 UAS, which also includes a canonical RSC motif (box). See Fig. S4 for comparison with profiles of cross-linked chromatin. (*B*) A subset of Gal4 UAS nucleosomes are insoluble. Chromatin landscapes showing all fragment sizes reveal high occupancy of the nucleosome over the Gal4 UAS in soluble chromatin after 2.5′ digestion, and this is replaced by subnucleosomal particles after 20′ digestion. Nevertheless, the pellet is strongly enriched for this nucleosome relative to the genome as a whole at both time points. This conclusion is confirmed by parsing the data into size classes, which shows that pellet enrichment is specific for the 111- to 140 bp size class. (*C*) V-plot of the 1-kb region surrounding the Gal4 UAS. See Fig. S4*B* for interpretation.

the RSC at the Gal4 UAS can make transcription-factor binding sites more accessible (7), and we suggest that the insolubility of a fraction of these partially unwrapped nucleosomes is caused by transient nucleosome engulfment.

When this work was in progress, a study appeared that systematically documented the existence of >1,000 "fragile" nucleosomes throughout the *Saccharomyces cerevisiae* genome, mostly in regions previously thought to be "nucleosome-free" (9). We found a very close correspondence between our datasets and theirs, including eviction of the single nucleosome over the Gal4 UAS (Fig. S4*A*). Therefore, many nucleosomes become catastrophically evicted as a result of MNase digestion. Eviction is not eliminated by standard formaldehyde cross-linking, because this treatment had no discernable effect at the Gal4 UAS (Fig. S4*A*).

Fragment Midpoint vs. Length Maps of Nucleosomes and Subnucleosomal Particles. Occupancy maps do not take into account fragment-size information that is obtained from mapped paired-end reads, and grouping mapped fragments by size recovers only gross differences. To recover all fragment-size information, we devised a simple DNA fragment midpoint mapping procedure akin to dot plots used for sequence alignments, in which a dot is placed on a 2D map for each datapoint. In a fragment midpoint

vs. length map, the *x* axis represents the map position and the *y* axis the fragment length, and a dot is placed on the map for each fragment (Fig. S4*B*). When we applied this procedure to the Gal1-Gal10 region, we observed a regular series of dot clusters corresponding to phased nucleosomes, which decreased in protected DNA length from 2.5 to 20 min (Fig. 3*C*). In the case of the nucleosome over the Gal4 UAS, the dot cluster is V-shaped, with a vertex at ~110 bp. Each sharp edge of the V represents a fragment cleaved precisely on one side of the nucleosome and on the other side beyond the nucleosome, and the vertex represents the limit digest, where MNase has cleaved precisely on both sides of the nucleosome. In this way, midpoint mapping can be used to precisely define the minimal region protected from MNase digestion by this well-positioned nucleosome. In contrast, most nucleosomes on either side are detected as more diffuse clusters of dots ~140 to 160 bp in length, indicating either dynamic wrapping/unwrapping during MNase digestion, or weaker positioning, or both.

Chromatin Mapping of Transcription-Factor Binding Sites. We next applied our fragment midpoint vs. length mapping strategy to characterize the binding features of known transcription factors in their native state. We used published binding site calls for low-resolution ChIP data combined with motif analysis to precisely align all regions of the genome bound by a transcription factor around the consensus motif (10). Midpoint vs. length plots (V-plots) were constructed either by combining the 2.5- and 20-min data or by finding the difference between them. The maps for Abf1 are shown together with an interpretive diagram (Fig. 4). As a negative control, we constructed V-plots of consensus motifs not bound by Abf1 (Fig. S5). Several features are evident. The minimal protected region is mapped on the *y* axis as the point where the central diagonals intercept and on the *x* axis by extrapolating the diagonals (red) that border the gap to $y = 0$. Abf1 has a bipartite DNA-binding motif (RTCAYTnnnnACGW), so the line of dots within the gap likely represents preferential MNase cleavages within the 4-bp nonspecific segment. Conspicuously phased nucleosomes are seen on either side of the aligned Abf1 binding sites with a 280-bp center-to-center spacing, ~100-bp wider than the genome-wide average. The rounded cluster of nucleosomal fragments after 2.5-min digestion flattens out after 20 min, suggesting limit protection at the edges of the 147-bp core. Satellite bands at ~130 bp and ~90 bp that appear after 20-min digestion indicate preferential internal cleavages of nucleosomes that flank depleted regions (11), and can account for the peaks seen in the global length distribution (Fig. 1).

Abf1 has been shown to be involved in phasing flanking nucleosomes (12, 13), presumably by recruiting ATP-dependent nucleosome remodelers. We note that the triangular shape of the subnucleosome-sized fragment densities, centered in between the flanking nucleosomes, indicates occupation of subnucleosome-sized particles distributed between Abf1 and the flanking nucleosomes on both sides. This pattern was especially conspicuous in the Abf1 V-plot constructed using a different MNase-digestion dataset (3), where the size distribution was biased toward shorter fragments (Fig. S6). To account for these distributed particles we speculate that they are nucleosome remodelers that occupy the extended linker regions on both sides of Abf1 and slide nucleosomes away from Abf1 to create nucleosome-depleted regions (14). This process would account for the direct centering of Abf1 between widely spaced flanking nucleosomes. Reb1 is also known to phase flanking nucleosomes (15), and it shows a similar pattern to that of Abf1, albeit with a smaller footprint seen as a lower vertex and narrower gaps (Fig. 5*A*). Cbf1 (Fig. 5*B*) and Rap1 (Fig. 5*C*) show weaker nucleosome phasing and less well-defined concentrations of subnucleosomal particles than for Abf1 and Reb1. Virtually identical maps were obtained using solubilized chromatin (Fig. S7).

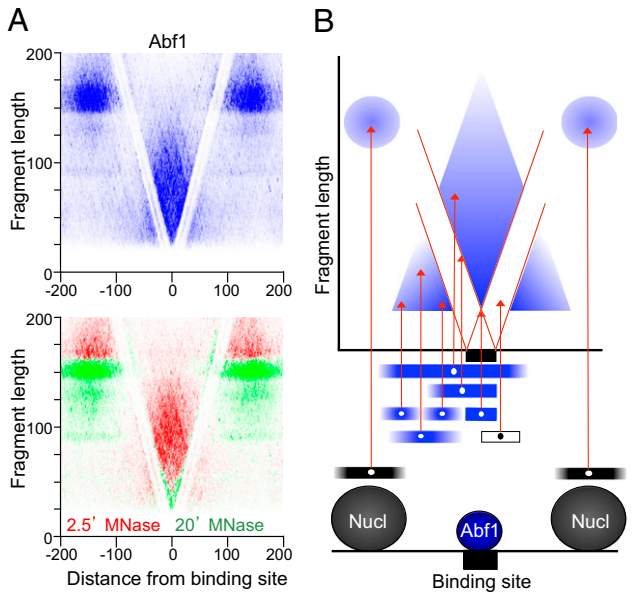

Fig. 4. V-plot of the Abf1 transcription factor. (*A*) Map of the 400-bp region spanning Abf1 transcription-factor binding sites is shown, where data are combined for the 2.5- and 20-min time points (*Upper*, blue), and differentially colored (*Lower*, red for 2.5 min and green for 20 min). Orientation is based on alignment with the Abf1 consensus motif. (*B*) Schematic diagram illustrates how the map is interpreted. Fragments are indicated below the graph. A fragment that spans a protected region (first blue fragment) results in a dot placed in the central sector (vertical red arrow). The left diagonal results from fragments cleaved precisely on the right side of the protected region (second blue fragment), and likewise for the right diagonal. The minimal protected region is at the intersection of the diagonals on the *y* axis, and is also represented as the width of the gap on the *x* axis (extrapolation of the diagonal red lines to $y = 0$), which in the case of Abf1 is 20 bp. The open box represents a fragment that is not observed because its left end is protected from cleavage. The flanking triangle densities are produced by protected fragments that are near or adjacent to Abf1 but are cleaved in between.

These maps are in excellent agreement with previous maps of these factors, where DNaseI hypersensitivity was shown to be maximal on either side of the DNA-binding motif (16). The common features of V-plots for these factors suggest that different DNA-binding proteins use similar mechanisms to position flanking nucleosomes on either side.

Transcription-factor V-plots also reveal contextual differences between binding sites. Whereas Abf1, Reb1, Cbf1, and Rap1 lie between phased nucleosomes, Sut1 (Fig. 5*D*) and Pho2 (Fig. 5*E*) show a uniform distribution of nucleosomes in their vicinity. The high contrast between the 2.5- and 20-min time points, as seen in the two-color plots, suggests that the regions around factors that phase nucleosomes are also highly sensitive to MNase digestion, whereas Sut1 shows lower contrast between time points, consistent with binding in both nucleosomal and nucleosome-depleted contexts. Moreover, Pho2 and Ume6 V-plots (Figs. 5 *E* and *F*) display highly unusual features relative to other transcription factors. For Pho2, the diagonals lie on the outside of the V gap, suggesting an especially strong barrier to neighboring particles. For Ume6, there is conspicuous asymmetry, with more protection from MNase on the upstream than the downstream side. Consistent with this observation, Ume6 has been shown to recruit the Isw2 ATP-dependent nucleosome remodeler, creating a nuclease-inaccessible region upstream of Ume6 binding sites, which is needed for repression of early meiotic genes (17). Thus, V-plots can provide insights into functional relationships between transcription factors and nucleosomes.

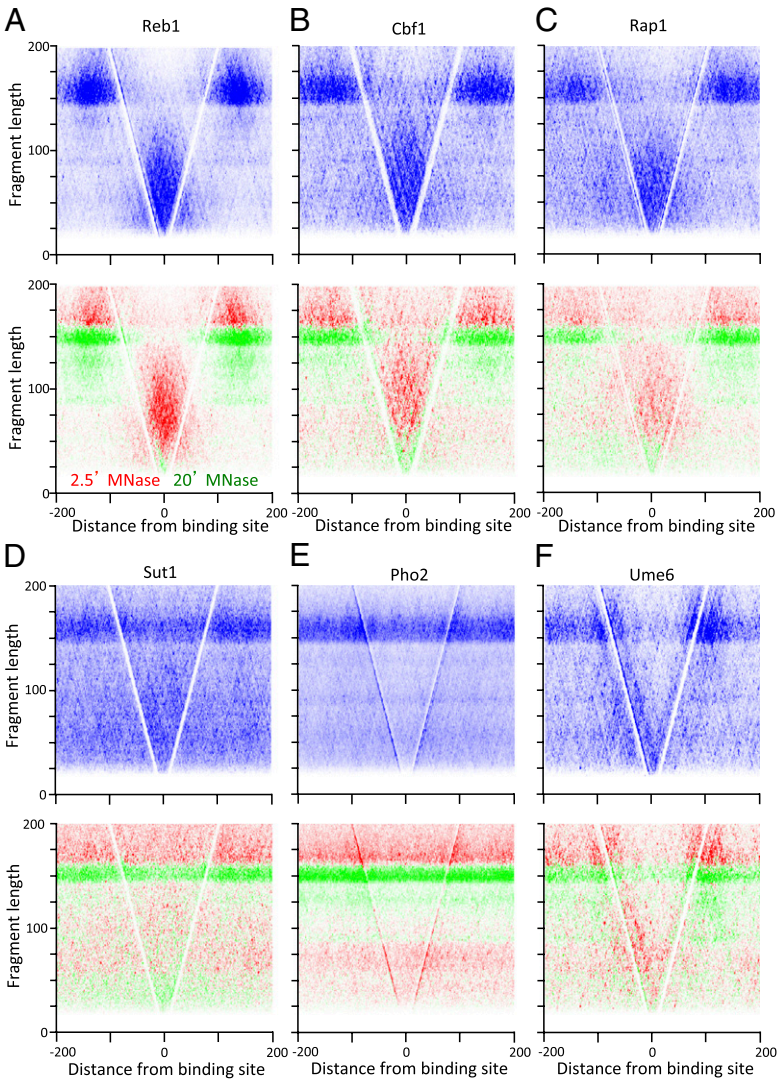

Fig. 5. V-plots of aligned transcription factor binding sites. See the legend to Fig. 4 for details (*A*–*F*) V-plots are shown for (*A*) Reb1, (*B*) Cbf1, (*C*) Rap1, (*D*) Sut1, (*E*) Pho2, and (*F*) Ume6. Similar V-plots were obtained for fragments from solubilized chromatin (Fig. S7).

Discussion

We have shown that the yeast epigenome, including nucleosomes, ATP-dependent remodelers, and transcription factors can be mapped at single base-pair resolution using traditional MNase treatment of unfixed nuclei followed by a simplified version of the Illumina paired-end sequencing protocol. By analyzing two different MNase digestion time points, together with occupancy and V-plots, we could infer dynamics, both for an unstable nucleosome and for regions around transcription factors. Although similar profiles were obtained from total nuclei, solubilized chromatin, and insoluble chromatin over most of the genome, our mapping of the insoluble nucleosome fraction has provided additional insights into nucleosome dynamics. The similar recovery of protected DNA fragments from both intact nuclei and solubilized chromatin implies that these native chromatin samples can be used directly for high-resolution ChIP, thus avoiding complications associated with formaldehyde cross-linking, such as epitope masking and reduced solubility (18, 19), and allowing for quantitative recovery from small amounts of cells or tissues.

Our method has several other advantages for chromatin profiling. The method is quantitative, in that all particles resulting from MNase digestion are measured in the same sample in a single experiment, regardless of size. Because MNase quickly digests linker regions but only slowly encroaches on nucleosomes and smaller particles, it can reveal nuclease sensitivity as a by-product of mapping nuclease-resistant particles. This feature is the inverse of DNaseI hypersensitivity mapping, which maps the sensitive sites and infers the presence of particles in between (16, 20, 21). Our method is highly scalable, can be applied to any cell type without the need for antibodies, tags, or disruptive treatments, and is suitable for application to larger genomes, where the isolation of the "active" chromatin fraction followed by paired-end sequencing has been used to map both nucleosomes and paused RNA polymerase II from *Drosophila* cells (2). As the number of base pairs per flow cell lane increases, the coverage of small particles deepens, making full epigenome sequencing especially cost-effective. In addition, all of our data were collected using only 25 cycles per end, which we have found suffices for the active chromatin fraction of genomes up to at least 15 times as large (22), thus lowering the cost and reducing machine time for epigenomic applications relative to genomic sequencing, where longer reads are the norm. In this way, MNase mapping of native chromatin is ideal for genome-wide chromatin profiling, producing the epigenomic equivalent of genomic sequencing projects,

where single base-pair resolution maps of entire genomes has provided the basic infrastructure for driving genetic biology over the past decade.

Experimental Procedures

Chromatin Isolation. *S. cerevisiae* cultures were grown in YEPD medium at 30 °C to OD_{600} = 0.8. Nuclei were prepared as previously described (4), flash-frozen in liquid nitrogen, and stored at −80 °C. Nuclei were thawed at room temperature and digested with MNase, followed by chromatin preparation as previously described (4), except that after MNase digestion, the slurry was passed four times through a 20-gauge needle, then four times through a 26-gauge needle (23), and the combined S1+S2 supernatants were clarified by centrifugation in a fixed-angle Sorvall SS34 rotator at 17,200 × *g* at 4 °C for 10 min at least twice or until no visible pellet remained.

Solexa Sequencing and Analysis. The standard Illumina paired-end library preparation protocol (Illumina # PE-930-1001) was used except as follows: (*i*) All Qiagen clean-up steps and gel purifications were omitted. (*ii*) Phenol/chloroform extraction was used to stop reactions followed by S300 spin column clean-up and Speed-vac volume reduction. (*iii*) Ampure XP bead steps following adapter ligation and PCR removed excess adapters and primers, respectively. (*iv*) Reaction volumes were 50 μL, except for the PCR amplification step, where the volumes were 10 to 25 μL. (*v*) PCR extensions were done at 60 °C to minimize bias against AT-rich sequences (24). (*vi*) Low-retention 1.5-mL (siliconized) microfuge tubes were used throughout, minimizing tube transfers to reduce losses. A detailed protocol (*SI Experimental Procedures*) has been used for 20 to 800 ng starting DNA from MNase-treated chromatin (based on Quant-it Picogreen fluorescence with RNase added). Cluster generation, followed by 25 rounds of paired-end sequencing in an Illumina HiSeq 2000, was performed by the Fred Hutchinson Cancer Research Center Genomics Shared Resource. After processing and base calling by the Illumina Eland program, reads with zero, one, or two mismatches were mapped to the yeast genome using Novoalign and default parameters, where each multiple hit was assigned to one site chosen at random. Solexa data analysis was performed as previously described (2), except that the fraction of mapped reads spanning each base-pair position was multiplied by the total number of base pairs mapped genome-wide to give a normalized count for that position.

V-Plot Construction. Transcription factor binding site locations were obtained from http://fraenkel.mit.edu/improved_map/p005_c2.gff (10). To generate comprehensive V-plots, paired-end reads from both the 2.5- and 20-min MNase digestion experiments were combined, and the length of each fragment was plotted as a function of the distance from the fragment midpoint to the center of the site for each annotated feature. Fragments greater than 200 bp were excluded. Heatmaps were generated by quantifying the number of reads at each relative distance and length coordinate. The maximum intensity of each heatmap was independently scaled to achieve the greatest contrast. The red-green V-plots were generated in a similar fashion, except that the reads from the 2.5- and 20-min MNase digestions were normalized for sequence depth and the difference in signal between the two experiments was plotted for each relative distance and length coordinate. In each difference V-plot, we enumerated the number of reads at each fragment-length midpoint location from each digestion time. The location was colored depending on which dataset contained more reads: green for the 2.5 min, red for the 20 min, white for no difference. Comprehensive V-plots for all 118 transcription factors analyzed in this study are provided in Fig. S8 and summary statistics are listed in Table S1.

ACKNOWLEDGMENTS. We thank Andy Marty and Jeff Delrow of The Fred Hutchinson Cancer Research Center Genomics Shared Resource for helpful discussions on Illumina sequencing technology and protocols.

1. Noll M (1974) Subunit structure of chromatin. *Nature* 251:249–251.
2. Weber CM, Henikoff JG, Henikoff S (2010) H2A.Z nucleosomes enriched over active genes are homotypic. *Nat Struct Mol Biol* 17:1500–1507.
3. Kent NA, Adams S, Moorhouse A, Paszkiewicz K (2011) Chromatin particle spectrum analysis: A method for comparative chromatin structure analysis using paired-end mode next-generation DNA sequencing. *Nucleic Acids Res* 39:e26.
4. Furuyama S, Biggins S (2007) Centromere identity is specified by a single centromeric nucleosome in budding yeast. *Proc Natl Acad Sci USA* 104:14706–14711.
5. Henikoff S, Henikoff JG, Sakai A, Loeb GB, Ahmad K (2009) Genome-wide profiling of salt fractions maps physical properties of chromatin. *Genome Res* 19:460–469.
6. Li G, Levitus M, Bustamante C, Widom J (2005) Rapid spontaneous accessibility of nucleosomal DNA. *Nat Struct Mol Biol* 12:46–53.
7. Floer M, et al. (2010) A RSC/nucleosome complex determines chromatin architecture and facilitates activator binding. *Cell* 141:407–418.
8. Lorch Y, Maier-Davis B, Kornberg RD (2006) Chromatin remodeling by nucleosome disassembly in vitro. *Proc Natl Acad Sci USA* 103:3090–3093.
9. Xi Y, Yao J, Chen R, Li W, He X (2011) Nucleosome fragility reveals novel functional states of chromatin and poises genes for activation. *Genome Res* 21:718–724.
10. MacIsaac KD, et al. (2006) An improved map of conserved regulatory sites for *Saccharomyces cerevisiae*. *BMC Bioinformatics* 7:113.
11. Tolstorukov MY, Kharchenko PV, Goldman JA, Kingston RE, Park PJ (2009) Comparative analysis of H2A.Z nucleosome organization in the human and yeast genomes. *Genome Res* 19:967–977.
12. Bai L, Ondracka A, Cross FR (2011) Multiple sequence-specific factors generate the nucleosome-depleted region on CLN2 promoter. *Mol Cell* 42:465–476.
13. Ganapathi M, et al. (2011) Extensive role of the general regulatory factors, Abf1 and Rap1, in determining genome-wide chromatin structure in budding yeast. *Nucleic Acids Res* 39:2032–2044.
14. Whitehouse I, Tsukiyama T (2006) Antagonistic forces that position nucleosomes in vivo. *Nat Struct Mol Biol* 13:633–640.
15. Hartley PD, Madhani HD (2009) Mechanisms that specify promoter nucleosome location and identity. *Cell* 137:445–458.
16. Hesselberth JR, et al. (2009) Global mapping of protein-DNA interactions in vivo by digital genomic footprinting. *Nat Methods* 6:283–289.
17. Goldmark JP, Fazzio TG, Estep PW, Church GM, Tsukiyama T (2000) The Isw2 chromatin remodeling complex represses early meiotic genes upon recruitment by Ume6p. *Cell* 103:423–433.
18. Schmiedeberg L, Skene P, Deaton A, Bird A (2009) A temporal threshold for formaldehyde crosslinking and fixation. *PLoS ONE* 4:e4636.
19. van Steensel B (2005) Mapping of genetic and epigenetic regulatory networks using microarrays. *Nat Genet* 37 (Suppl):S18–S24.
20. Shibata Y, Crawford GE (2009) Mapping regulatory elements by DNaseI hypersensitivity chip (DNase-Chip). *Methods Mol Biol* 556:177–190.
21. Weintraub H, Groudine M (1976) Chromosomal subunits in active genes have an altered conformation. *Science* 193:848–856.
22. Teves SS, Henikoff S (2011) Heat shock reduces stalled RNA Polymerase II and nucleosome turnover genome-wide. *Genes Dev*, in press.
23. Jin C, Felsenfeld G (2007) Nucleosome stability mediated by histone variants H3.3 and H2A.Z. *Genes Dev* 21:1519–1529.
24. López-Barragán MJ, et al. (2011) Effect of PCR extension temperature on high-throughput sequencing. *Mol Biochem Parasitol* 176:64–67.